BNL, 1995

An influence of a tile/fiber assemblies characteristics on the performance of the STAR EMC, and possible methods of the EMC calibration.

A.A.Derevschikov and O.D.Tsai

Institute for High Energy Physics

Protvino Russia

Abstract

We discuss the influenence of a tile/fiber assemblies characteristics on the performance of the Electromagnetic Calorimeter for the STAR detector. A global characteristics of the whole calorimeter defined from the Monte-Carlo simulation were presented. A different methods of the calorimeter calibration were discussed.

Introduction

A description of the proposed sampling lead/scintillator Electromagnetic Calorimeter (EMC) for the STAR detector can be found in [1]. Similar calorimeters are build and planned for a lot of experiments SDF, SDC, ZEUS, ATLAS and others. In this report we try to use the experience of a people working under that projects to find the characteristic of the planned STAR EMC. Our goal was to investigate the influence of the tile/fiber assemblies characteristics on the performances of the EMC. It is important to define the requirement on the minimum light yield from the tile/fiber assemblies and a level of the tile-to-tile nonuniformity before choose the final option for the tile/fiber assemblies. We discuss different methods of the EMC calibration because the quality control requirements for a tile/fiber elements, in the final case, depends on the calibration procedure.

Usually, the energy resolution of the calorimeter is parametrized by:

$$\frac{\sigma}{\mathbf{E}} = \frac{\mathbf{a}}{\sqrt{\mathbf{E}}} \oplus \mathbf{b} \tag{1}$$

The first term comes from sampling fluctuation and photostatistics. The second term comes mainly from tile-to-tile responce nonuniformity. The influence of the systematic effects on the second term at very high energies can be found in [2]. The requirements for the STAR EMC was the energy resolution should be better than **20 %** at an energies above the **1 GeV**.

To determine the minimum light yield requirements in the EMC we will describe the light yield of a single scintillation tile in terms of the number of photoelectrons per minimum ionizing particle ($\mathbf{N_{phe/mip}}$). In this report we omit the discussion about: particular design of the tile/fiber assemblies, choosing materials for scintillating tiles, wavelength-shifting fibers and surface reflector on tiles which are defines the absolute light yield from the tile/fiber assemblies.

To include more ore less true level of the tile-to-tile nonuniformity in the Monte-Carlo simulation it is useful to consider a sources of a relative light yield variation from the tile/fiber assemblies. A detailed description a varios contribution to the tile-to-tile light yield variation can be found in [3], the quality control studies for the CDF End Plug Upgrade Hadron Calorimeter. In our calculation we are going to use a some results of the CDF quality control studies [3] and a results of the production of a scintillation tiles for the ATLAS hadron calorimeter. We are refer to the ATLAS because they use a technology for the production of a scintillation tiles similar to the proposed for the STAR EMC tiles production.

In general, the total variation of the relative tile/fiber light yield distribution can be define as:

$$\sigma_{\mathbf{tot}} = \sigma_{\mathbf{fib}} \oplus \sigma_{\mathbf{tile}} \oplus \sigma_{\mathbf{other}} \tag{2}$$

where a $\sigma_{\mathbf{fib}}$ is the relative fiber light yield variation, a $\sigma_{\mathbf{tile}}$ is the average tile light variation and, a $\sigma_{\mathbf{other}}$ corresponds to the light yield variation due to other factors.

The $\sigma_{\mathbf{fib}}$ describe a factors such as: quality of the fiber mirroring, quality of the fiber splicing, variation in the diameter of the WLS fiber and, quality of fibers assembling into mass-terminated connectors. The $\sigma_{\mathbf{fib}}$ equal **3.2 %** was determined during the quality control tests for the CDF End Plug Upgrade Hadron Calorimeter [3]. As we are going to use similar technics for the fiber preparation we expect that the $\sigma_{\mathbf{fib}}$ for the STAR EMC will be close to measured in CDF.

The $\sigma_{\mathbf{tile}}$ comes from: a variation in the thickness of scintillation tiles, a variation in the absolute light yield, and a quality of the mechanical preparation of a tiles. We expect the $\sigma_{\mathbf{tiles}}$ for STAR EMC will be close to **5.0** % as determined during a monitoring of the ATLAS hadron calorimeter. Our conclusion based on the private communication with a people from the ATLAS, see also [4]. The variation in the tile light yield, largest compare to CDF, comes, mainly from the largest variation in the tile thickness and a variation in the absolute light yield. Last was connected with the quality of the initial polysterene for the tile production by an injection molding procedure.

The $\sigma_{\mathbf{other}}$ depends of the particular EMC design and technology of the EMC towers assembling, and for this reason difficult estimated for us. For the purpose of this calculation we refer to the CDF results [3], and apply $\sigma_{\mathbf{other}}$ equal **3.7**%.

Summarize all the above contribution to the variation of the relative tile light yield we estimate the $\sigma_{\mathbf{tot}}$ close to **7.0**% will be achiveble for the STAR EMC, *if an appropriate quality control tests will be performed for the EMC components.*

Monte Carlo simulation

The EGS4 program [5] was used to simulate an electromagnetic showers produced in a tower by an electron and photon beam at twenty values of the incident energy from the **0.3 GeV** up to **26 GeV**. A one thousand showers were generated for the each energy point. The incident beam direction was perpendicular to the tile surface. The energy cuts for an electrons was **90 KeV** and **600 KeV** for gammas.

The calorimeter tower considered in the simulation program consisted of a stack of alternative layers of a plastic scintillator plate and a lead plate. The tower was composed from **18** alternative layers. The thickness of the lead plate - **0.53 cm** and **0.4 cm** for the scintillator. The plate considered infinit in tne transversal direction. The **Al** plate with the thickness **2.0 cm** inserted just before the first layer. A particles initiated shower started in an air at the normal condition at the distance **230.0 cm** from the surface of the **Al** plate. The shower maximum detector don't included in this computation.

The result of the EGS4 simulation for the single shower was a set of the energy deposition $(\mathbf{E_i}, \mathbf{i} = \mathbf{1}, \mathbf{18})$ in the each of the scintillation tile. The tile-to-tile nonuniformity and photostatistic included in the calculation by the next way:

- for the $\mathbf{j^{th}}$ tower of the EMC a set of a coefficient $(\mathbf{C_i^j}, \mathbf{i} = \mathbf{1}, \mathbf{18})$ were generated in acoordance with:

$$\mathbf{C_i^j} = \mathbf{1} + \sigma_{\mathbf{tot}} \cdot \mathbf{r_i^j} \tag{3}$$

  where $\mathbf{r_i^j}$ is a random number generated according to the standard Gaussian distribution, and $\sigma_{\mathbf{tot}}$ is the total variation of the relative light yield from the tile/fiber assemblies.

- the energy deposition $\mathbf{E_i}$ in the $\mathbf{i^{th}}$ tile of the $\mathbf{j^{th}}$ tower weighted by the corresponding coefficient $\mathbf{C_i^j}$

- to convert weighted energy deposition in the tile to the signal from a photomultiplier a random integer number **Np** generated accordin to the Puasson law with the mean μ

which is determined from:

$$\mu = \frac{\mathbf{C^j_i E_i}}{\overline{\mathbf{E}}_{\mathbf{mip}}} \mathbf{N_{phe/mip}} \tag{4}$$

where $\overline{\mathbf{E}}_{\mathbf{mip}}$ is the mean energy deposition in the tile from the minimum ionizatin particle, and $\mathbf{N_{phe/mip}}$ is the number of photoelectrons per minimum ionizing particle.

- a photomultiplier amplification included by generation a random number $\mathbf{Ng}$ according to a Gaussian law with the mean $\mathbf{Np}$ and standard deviation $\sigma_{\mathbf{Np}} = \mathbf{0.01} \cdot \mathbf{Np}$.
- a 'real signal' from a tower was determined by summarize signal from a tiles composed this tower.

$$\mathbf{S} = \sum_{\mathbf{i}}^{\mathbf{18}} \mathbf{Ng} \tag{5}$$

This procedure was used to compute the 'real signal' from the each individual tower to the each simulated event.

A some comments are necessary for the presented above procedure to estimate the 'real signal' from the tower. We use a single coefficient to characterize the tile/fiber assemblies nonuniformity instead of a function of the coordinates $(\mathbf{x,y})$ on the surface of the tile, because some ways exist to reduce the tile response nonuniformity across the surface, such as a usage of an appropriate fluttening mask. We also omit a lot of systimatic effects such as an influense of the magnetic field on the light yield from the tile/fiber assemblies, the dependence of the light yield from the tile/fiber assemblies vs the tile size, an electronic noise, and others, that may significant influense on the EMC performance.

Results

Under the global characteristics of the EMC we understand the calorimeter response and calorimeter energy resolution obtained over the all towers, that were composed EMC. In oder to define a global characteristic of the whole EMC we compute the 'real response' from a $\mathbf{1000}$ different towers. The each tower characterized by its own set of a coefficients $\mathbf{C^j_i}$. A coefficients for a tower were generated for a four values of the $\sigma_{\mathbf{tot}} : \mathbf{0.07}, \mathbf{0.1}, \mathbf{0.15}, \mathbf{0.2}$. The photostatistic included in the calculation by applying the $\mathbf{N_{phe/mip}} : \mathbf{0.5}, \mathbf{1.0}, \mathbf{1.5}, \mathbf{2.0}$.

Notation

- A mean 'real signal' from a $\mathbf{k^{th}}$ tower $\mathbf{Sm_k}$ was defined as:

$$\mathbf{Sm_k} = \frac{\mathbf{1}}{\mathbf{N}} \sum_{\mathbf{i}}^{\mathbf{1000}} \mathbf{S_i} \tag{6}$$

where $\mathbf{N}$-number of simulated showers.

- A mean EMC response **Semc** was defined as:

$$\mathbf{Semc} = \frac{\mathbf{1}}{\mathbf{K}} \sum_{\mathbf{k}}^{\mathbf{1000}} \mathbf{Sm_k} \tag{7}$$

  where **K**-number of a towers composed the EMC.

- A mean EMC energy resolution **Remc** was defined as:

$$\mathbf{Remc} = \frac{\mathbf{1}}{\mathbf{K}} \sum_{\mathbf{k}}^{\mathbf{1000}} \mathbf{Rt_k} \tag{8}$$

  where $\mathbf{Rt_k}$ - energy resolution for the $\mathbf{k^{th}}$ tower, defined for the case of the absolute calibration of the each tower at the each energy of the incident electron.

Calorimeter response

At first, we are iterested how the nonuniformity and photostatistic influenses on the distribution of the mean 'real signal' from a towers. The Figure 1.a shows the mean EMC response with the $\sigma_{\mathbf{tot}} = \mathbf{0.1}$ for a different photostatistics. The bars on the data points on this figure are not an errors in the determination of the mean EMC response but rather the rms deviation of the distribution of the mean 'real signal' from a towers. The energy leakage from the EMC at high energy can be seen here , the more presentative energy leakage will be seen in Fig.3.

Figure 1.b and Fig. 1.c shows the ratio of the standard deviation to the mean value of the distribution of the mean 'real signal' for a different $\sigma_{\mathbf{tot}}$ with the $\mathbf{N_{phe/mip}} = \mathbf{1.0}$, and for a different photostatistics with the $\sigma_{\mathbf{tot}} = \mathbf{0.1}$, respectively. A nonuniformity affects the mean 'real signal' distribution by an increase of its width, only, while the mean value remains constant and distribution itself remains Gaussian. The σ/μ of this distribution behave like $\sim \mathbf{1}/\sqrt{\mathbf{12}}\sigma_{\mathbf{tot}}$ at the energy higher **2 GeV**. That is pointed, that, the tower mean 'real signal' depends on the response of a $\sim \mathbf{12}$ tiles, in average . The photostatistics don't influense significantly on the parameters of the distribution of the mean 'real signal'. For illustrative purposes, the distribution of the mean 'real signal' **Sm** from a towers for a different energy of an incident electrons and for a different tile/fiber assemblies nonuniformity presented in Fig. 2.

The proposed EMC have a full depth $\sim \mathbf{18}$ radiation lenghts, only. It is lead to a longitudinal energy leakage from the EMC at high energy. Figure 3.a and 3.b shows the mean EMC respons normalized to the energy of the incident electron and photon respectively. Where the $\mathbf{E_{rec}}$ was defined as $\mathbf{E^e_{rec}} = \mathbf{K} \cdot \mathbf{Semc^e}$ and $\mathbf{K} = \mathbf{1.0(GeV)/Semc^{1.0GeV}}$ was a calibration coefficient determined from the electron data. The shower longitudinal profile slowly depends on energy, like logaritmic type, therefore it was also expected for the $\mathbf{E/E_{rec}}$ value to depend on energy in the same manner. Form this figure clearly see, that at an energy close to **30GeV** the mean energy leakage rise up to $\sim \mathbf{4\%}$ in the case of an electron initiated showers, and up to $\sim \mathbf{6\%}$ for a showers comes from a photons.

Energy resolution

To define the requirement on the minimum light yield from the tile/fiber assemblies, we restrict the energy range up to $\mathbf{4\ GeV}$, to avoid longitudinal energy leakage from the EMC, and investigate the dependence of the EMC mean energy resolution for the case $\sigma_{\mathbf{tot}} = \mathbf{0.1}$ for a different light yield from the tile/fiber assemblies $\mathbf{N_{phe/mip}}$; $\mathbf{0.5}, \mathbf{1.0}, \mathbf{1.5}, \mathbf{2.0}$. Figure 4. shows the mean EMC energy resolution (**Remc**) fitted by:

$$\frac{\sigma}{\mathbf{E}} = \frac{\mathbf{p1}}{\sqrt{\mathbf{E}}}\sqrt{\mathbf{1} + \frac{\mathbf{p2}}{\mathbf{N_{phe/mip}}}} \oplus \mathbf{p3} \tag{9}$$

where the **p1** characterises the influense of a sampling and nonuniformity, and the **p2** included to substract the influense of the photostatistics. From this figure well see, the energy resolution defined by sampling and nonuniformity phenomena behave like $\sigma/\mathbf{E} = \mathbf{0.147}/\sqrt{\mathbf{E}}$, and when photostatistics taking into account the energy resolution well described by the:

$$\frac{\sigma}{\mathbf{E}} = \frac{\mathbf{0.147}}{\sqrt{\mathbf{E}}}\sqrt{\mathbf{1} + \frac{\mathbf{0.6}}{\mathbf{N_{phe/mip}}}} \tag{10}$$

The similar result obtained in [6]. As it follows from the above result *the light yield from the tile/fiber assemblies should be no worse* **0.7 phe/mip** *for the STAR EMC design requirement.*

In the real case the nonuniformities are statistically distributed and a different values of the energy resolution are obtained for a different towers. The nonuniformity affects the energy resolution distribution in two ways; by shift the mean value and by an increase of its width, while the distribution itself remains Gaussian. For illustrative, Fig 5. shows the distribution of the energy resolution for the whole EMC at a different energies and nonuniformity for the $\mathbf{N_{phe/mip}} = \mathbf{1.0}$.

The mean EMC energy resolution **Remc** in the energy range from **0.3 GeV** to **26.0 GeV** fitted by **(1)** for a different $\sigma_{\mathbf{tot}}$ and $\mathbf{N_{phe/mip}} = \mathbf{1.0}$ shown in Fig. 6. To find the influense of the $\sigma_{\mathbf{tot}}$ on the **a**-term, it was fitted by:

$$\mathbf{a} = \mathbf{a_0} \oplus \mathbf{a_1}\sigma_{\mathbf{tot}} \tag{11}$$

Where the $\mathbf{a_0}$ characterizes a sampling and photostatistics. A similar approach can be found in [2]. By taking into account the result (10), we may describes the mean EMC energy resolution by:

$$\frac{\sigma}{\mathbf{E}} = \frac{\mathbf{0.1445}\sqrt{\mathbf{1} + \frac{\mathbf{0.6}}{\mathbf{N_{phe/mip}}}} \oplus \mathbf{0.22}\sigma_{\mathbf{tot}}}{\sqrt{\mathbf{E}}} \oplus \mathbf{0.013} \tag{12}$$

To complete the description of the distribution mean 'real signal' and the tower energy resolution, on the Fig. 7.a shown the ratio σ/μ of the distribution of the tower energy resolution for a different $\sigma_{\mathbf{tot}}$ and the $\mathbf{N_{phe/mip}} = \mathbf{1.0}$, and Fig. 7.b shows the coefficient correlation **R** between the **Sm** and **Rt**.

Calibration

In the previos section the global characteristic of the EMC were determined for the case of the absolute calibration. It's means, correspondance between the energy deposition and the energy of the incident electron are known for the each tower of the EMC.

In practics, the absolute calibration of the each tower is very expansive, because needed a lot of the test beam time. The performance of the EMC for the case of the calibration of the each tower at one energy point can be found in [2]. Usually, a test towers, only, absolute calibrated on the test beam. And then, this information and a diffirent procedure were used to establish the correspondance between the energy deposition and the energy of the incident particle for the particular tower, characterized by its own set of the tile/fiber assemblies, a photomultipluer, and a channel of a readout electronics.

A lot of methods developed to find this correspondance. A recent publication of a results of ZEUS monitoring system with the usage of Cosmic Ray Muons [7] and $\mathbf{^{60}Co}$ sources [8], and ATLAS monitoring system with the $\mathbf{^{137}Cs}$ sources [4], gives a good example of a solution of this problem. Both ZEUS and ATLAS used the radioactive sours to scan the each scintillation tile. This method prowides:

- A possibility to perform the tower-to-tower equalization.
- A possibility to carry the absolute calibration from the test beam data.
- A possibility to control the quality of the optical components of the EMC.
- A possibility to monitor long term stability of the EMC components.

A published results of a reproducibility tests [8] [4], indicates that the source can be used as a gain monitor at the percent level. Howere as pointed in the above citation, usage of the radioactive sources as a primary calibration tool is limited, if frequent use is needed or if the calorimeter are very large due to the great time consuming.

In this section we compare a results of the calibration of the EMC with a cosmic ray muons and a $\mathbf{^{137}Cs}$ sources, taking into account the result of a measurements of a 'test towers' on the test beam. The suggestion have been the following:

- A test beam results provide information about the correspondance between the energy deposition in the 'test tower' and the energy of the incident electron. The $\sigma_{\mathbf{tot}} = \mathbf{0.0}$ for the tile/fiber assemblies composed 'test towers'. Obviously, in this case the result should look like on Fig. 1.a for the mean EMC responce. For the simplisity, to find the energy of the incident electron we use:

  $$\mathbf{E_{inc}} = \mathbf{a_1} + \mathbf{a_2 S} + \mathbf{a_3 S^2}, \tag{13}$$

  where $\mathbf{S}$ determined at equ. (5), and a coefficients $\mathbf{a_1}, \mathbf{a_2}, \mathbf{a_3}$ were determined from the fit (13) of the data shown on Fig. 1a.

- The $\mathbf{^{137}Cs}$ source will be moved in a guide tubes. The guide tube will be incorporated into the middle of the one of a lead plate, to provide the source positioning along the EMC supermodule. A induced current will be measured on the center of the each of the tower, composed supermodule. In this scheme only a part of a scintillations plate composed tower will provide a significant signal (in this computation we take into account eight scintillation plates, a four plates from the each side of the lead plate, in the which guide tube was installed). The $\mathbf{E_{inc}}$ determined from the equ. (13) corrected for the each tower and for the each event by comparing a responses of the 'test tower' and a current tower from the muons or $\mathbf{^{137}Cs}$, by the next way:

$$\mathbf{E^{\mu}_{inc}} = \mathbf{K_{\mu} E_{inc}} \tag{14}$$

$$\mathbf{E^{Cs}_{inc}} = \mathbf{K_{Cs} E_{inc}}, \tag{15}$$

where $\mathbf{K_{\mu}}$ for the $\mathbf{j^{th}}$ tower was calculated as:

$$\mathbf{K_{\mu}} = \frac{\mathbf{18}}{\sum_{\mathbf{1}}^{\mathbf{18}} \mathbf{C^{j}_{i}}} \tag{16}$$

and $\mathbf{K_{Cs}}$ for the $\mathbf{j^{th}}$ tower was calculated as:

$$\mathbf{K_{Cs}} = \frac{\sum_{\mathbf{1}}^{\mathbf{18}} \mathbf{w_i}}{\sum_{\mathbf{1}}^{\mathbf{18}} \mathbf{w_i C^{j}_{i}}}, \tag{17}$$

where a coefficients $\mathbf{w_i}$ depends on the location of the guide tube. A coefficients $\mathbf{w_i}$ were determined from the EGS4 simulation, as a relaitive energy deposition in a scintillation tiles, composed EMC tower, from a photons with the energy **0.662 MeV** started at normal direction to the surface of the plate. A soft electron component from the $\mathbf{^{137}Cs}$ source was considered catted in a lead surrounded guide tube.

- The current induced by a sources in the $\mathbf{j^{th}}$ was determined as:

$$\mathbf{I^{j}_{Cs}} = \sum_{\mathbf{1}}^{\mathbf{18}} \mathbf{w_i C^{j}_{i}} \tag{18}$$

- The signal from a muons was determined as:

$$\mathbf{I^{j}_{\mu}} = \sum_{\mathbf{1}}^{\mathbf{18}} \mathbf{C^{j}_{i}} \tag{19}$$

At first, we was interested how correlates the signal from a muons and induced carrent from a $\mathbf{^{137}Cs}$ sources with the mean 'real signal' from the tower. Figure. 8 shows the correlation between the mean 'real signal' from a tower **Sm** and the induced current $\mathbf{I_{Cs}}$ from the $\mathbf{^{137}Cs}$ source for a different location of the guide tubes in the EMC supermodule, and Fig. 9 shows the correlation for the case of the cosmic ray muons.

Obviously, when the single guide tube, incorporated in a one of the lead plate of the EMC supermodule, was used, a total energy correction for the tower cannot be achieved in a full energy range, because the mean shower longitudinal profile depends on energy and in consequence the different tiles relative contribution to the tower signal changes also with the energy. In addition, a coefficient $\mathbf{w_i}$ for a tiles are differ from the ideal case, because the best way is to take them in accordance with the mean shower profile. The all commented above refer to the muon calibration.

However, when we refer to the ZEUS results, it is useful take in mind that the design goal for the ZEUS was to reduce systematic errors to the level of less than **1%**. If the requirements for the STAR EMC not so strong, may be quit enough to use a more simple method of monitoring and calibration, as considered in this section.

As an illustration, Fig. 10 shows a distribution of the mean reconstructed energy in a towers of the EMC, corrected with the calibration from the muons (equ. (13), (14), (16)). A little shift of the mean value for the whole EMC comes from equ. (13), see also Fig. 3.a. Figure. 11 shows the σ/μ of this distribution for a different energy of a incident electrons, **(a)** - withought any calibration, **(b)** - with calibration from $\mathbf{^{137}Cs}$ source, and **(c)** - with calibration from muons. The position of the guide tube for the radioactive source correspond to the Fig. 8.b. The behaviour of the σ/μ on this figure follows from the comparision of a results shown on the Fig. 8.b and Fig. 9.

The Fig. 10. and Fig. 11. illustrate the possibility of a usage of the radioactive source and a cosmic ray muons to perform the tower-to-tower equalization and possibility to carry the absolute calibration by taking into account the absolute calibration of the 'test tower' on the test beam.

How it follows from the results shown on the Fig. 8.a, the usage of the $\mathbf{^{137}Cs}$ as a calibration tool may provide a better result compare to muons calibration, sometimes. As a illustration, Fig. 12. shows a result of correction by the $\mathbf{^{137}Cs}$ (hatched histogram) and muons (unhatched histogram) for the energy of incident electrons **0.3 GeV**; compare this result with the shown on Fig. 10.a.

If we will use two guide tubes incorporated into the lead plates with a numbers **6** and **9**, it will be possible to control a tiles from the $\mathbf{3^{th}}$ to the $\mathbf{12^{th}}$. The main contribution to the induced current comes from the $\mathbf{5^{th}}$ to the $\mathbf{10^{th}}$ tiles, in this case. By this way, a good correlation between current induced by radioactive source and mean 'real signal' from the tower will be achieveble in the wide energy range. The result shown on Fig. 9 (points with the label (b)) confirm the said above. Moreover, in this case it will be possible to control any mechanical damages in a central tile/fiber assemblies, which may occured during operation under a EMC supermodules.

To complite this discussion, lets compare an advanteges and a disadvanteges of the calibration and monitoring by a muons and rodioactive source, as it seems to us. A both methods, as a calibration tool, provide a similar results. The radioactive source method more faster compare to the calibration from a muons (as shown in [7] the relative calibration of the different modules can be obtained with an accuracy of about one percent for a measurement time of 3 - 5 days/module). In addition, the source method (in the case of a usage of a two guide tubes) will provide better control of the central tile/fiber assemblies. However, a problems may occured with the access to the EMC supermodule after its final positioning in the STAR detector. In view of this, the cosmic ray calibration may be performed during the STAR detector operation.

In general, situation looks like; before the installation of the EMC supermodule on the final position in the STAR detector, may be useful to scan them by radioctive source, and after the final installation perform calibration and monitoring by the cosmic ray.

The results of a fitting of the mean EMC energy resolution for the case of the discussed above methods of EMC calibration, shows that within the errors the obtained values of parameters **a** and **b**, coincide with the result (12).

We understand that the traditional fit (1), is not the best, for the case of the energy leakage from the EMC. We were used this fit to clarify the influence of the photostatistic and nonuniformity on the EMC resolution, only.

Conclusion

A global EMC characteristics determined from the Monte Carlo simulation were presented. The requirement on the absolute light yield from the tile/fiber assemblies was determined. The influence of the variation of the light yield from the tile/fiber assemblies on the EMC performance presented. A methods of the EMC calibration and monitoring with the ^{137}**Cs** radioactive source and cosmic ray muons were discussed.

We deeply thank **B.Tchouiko** *for the fruitful discussions during the preparation of this work.*

References

[1] *The STAR collaboration*, Conceptual Design Report for the Electromagnetic Calorimeter for the **STAR**, September 22, 1993.

[2] Budagov Ju. et al., JINR-? November 9, 1994.

[3] P.de Barbaro, K.Michaud, A.Bodek et al., Quality Control Studies of Scintillating Tile/Fiber Megatile Production for the CDF End Plug Upgrade Hadron Calorimeter., UR-1371/ER40685-821, September 30, 1994.

[4] F.Ariztizabal, M.Bosman, M.Cavala-Sforza et al., Construction and performance of an iron-scintillator hadron calorimeter with longitudinal tile configuration., NIM A 349 (1994).

[5] W.R.Nelson, H.Hirayama, D.W.Rogers., SLAC Report 165, Stanford, SLAC, 1985.

[6] A.Bodek and P.Auchincloss., Simple formylae for light-yield considerations in the design of Scintillator-Fe and scintillator-Pb sampling calorimeters., UR-1385/ER-40685-834, October 10, 1994.

[7] U.Behrens et al.., Calibration of the Forward and Rear ZEUS Calorimeter using Cosmic Ray Muons., DESY 93-121, August, 1993.

[8] U.Behrens, G.Golth, H.Kammerlocher et al.., Quality Control and Calibration of the ZEUS Forward and Rear Calorimeters with ^{60}Co Sources., DESY 92-064, May, 1992.

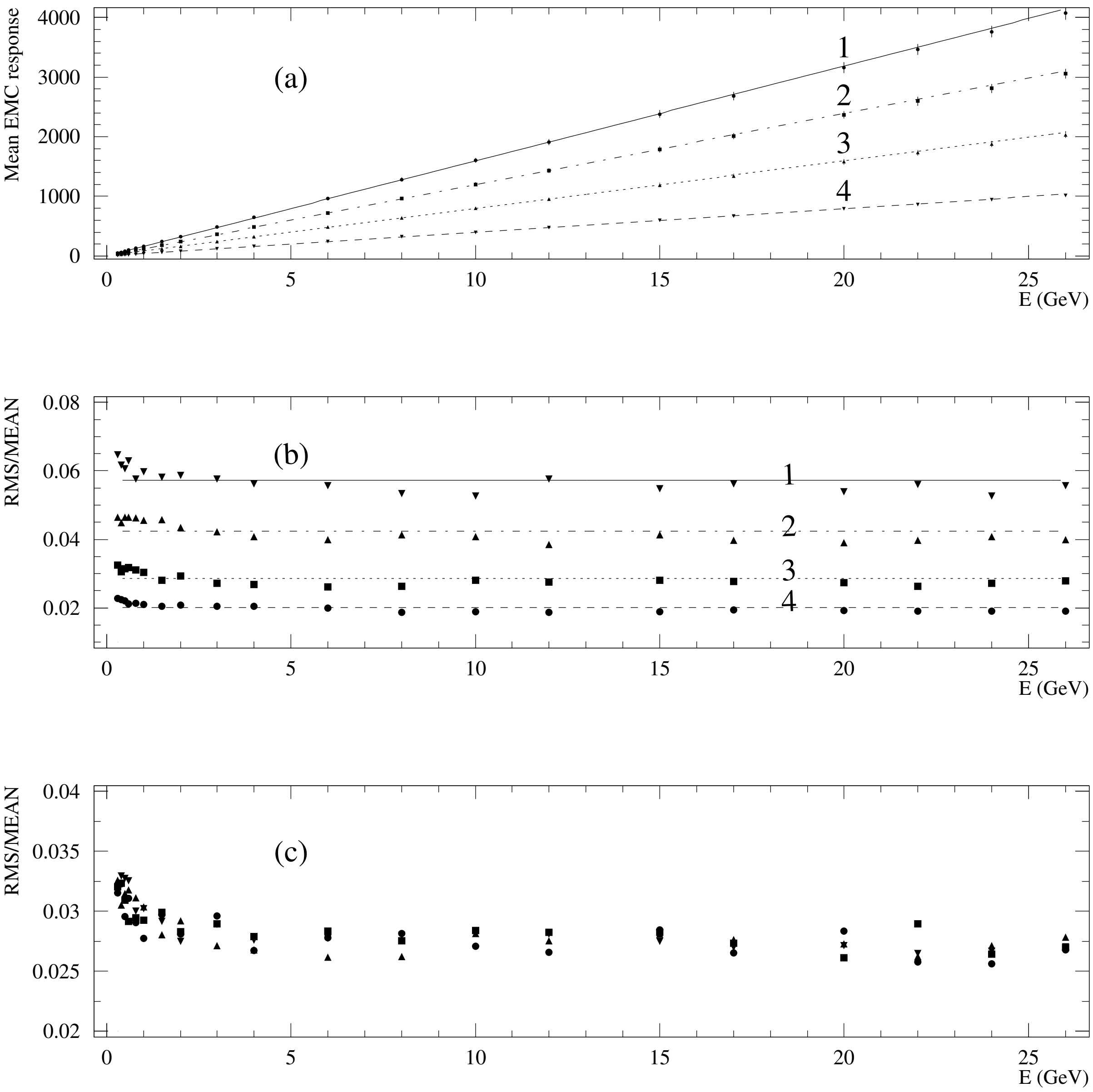

Figure 1: **(a).** The mean EMC response vs the energy of an incident electron, a **1, 2, 3, 4** correspond to $\mathbf{N_{phe/mip}}; \mathbf{0.5}, \mathbf{1}, \mathbf{1.5}, \mathbf{2}$, respectively. **(b).** The ratio of the standart deviation to the mean value of the distribution of mean 'real signal' from a towers. The $\mathbf{N_{phe/mip}} = \mathbf{1.0}$, and a **1,2,3,4** correspond to $\sigma_{\mathbf{tot}}; \mathbf{0.2}, \mathbf{0.15}, \mathbf{0.1}, \mathbf{0.07}$, respectively. **(c).** The ratio of the standart deviation to the mean value of the distribution of the mean 'real signal' from a towers. The $\sigma_{\mathbf{tot}} = \mathbf{0.1}$, and a different markers correspond to a different photostatistics.

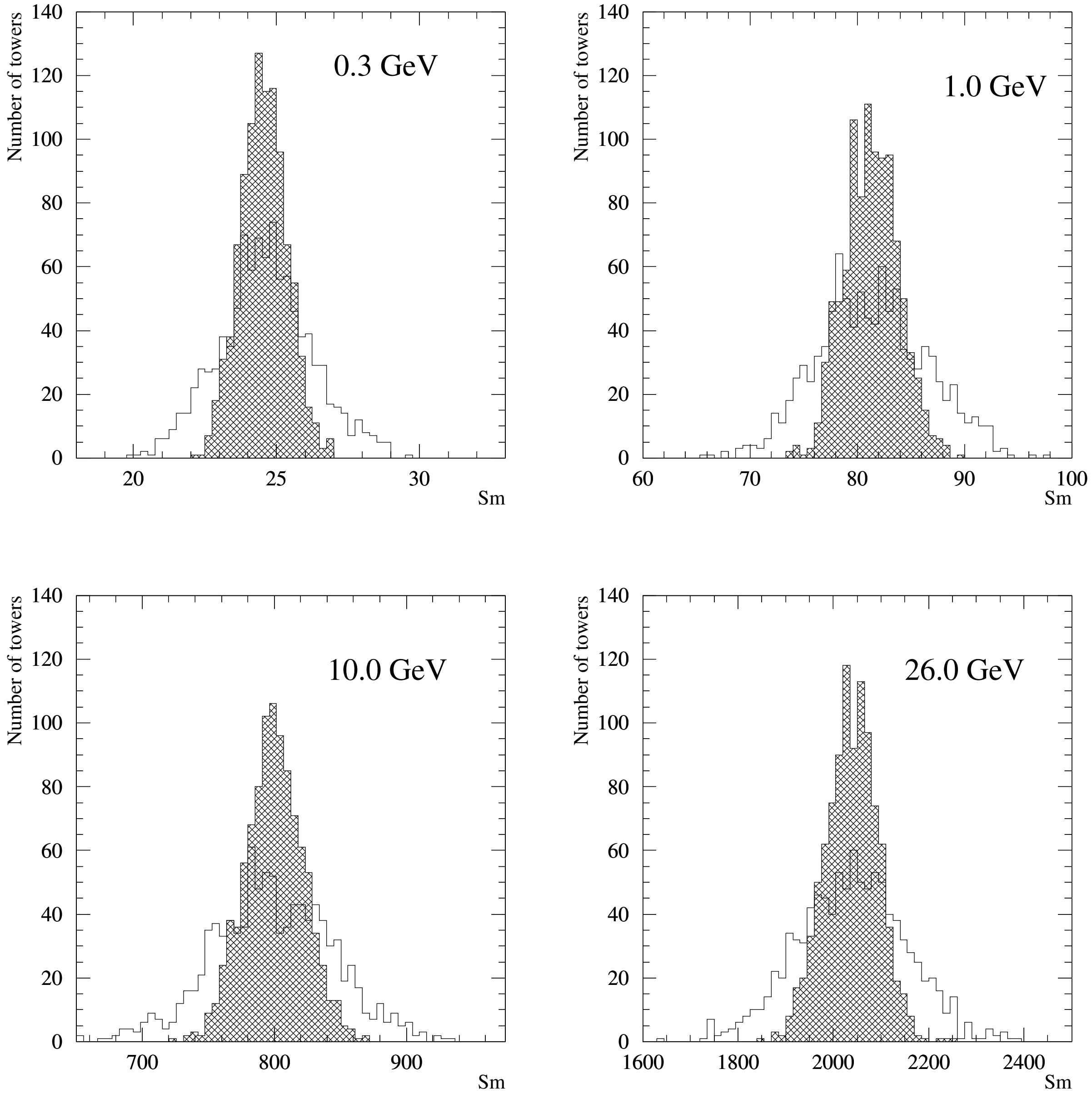

Figure 2: The distribution of the mean 'real signal' $\mathbf{Sm}$ from a towers. The $\sigma_{\mathbf{tot}} = \mathbf{0.1}$ and $\mathbf{0.2}$ correspond to a hatched and unhatched histograms, respectively.

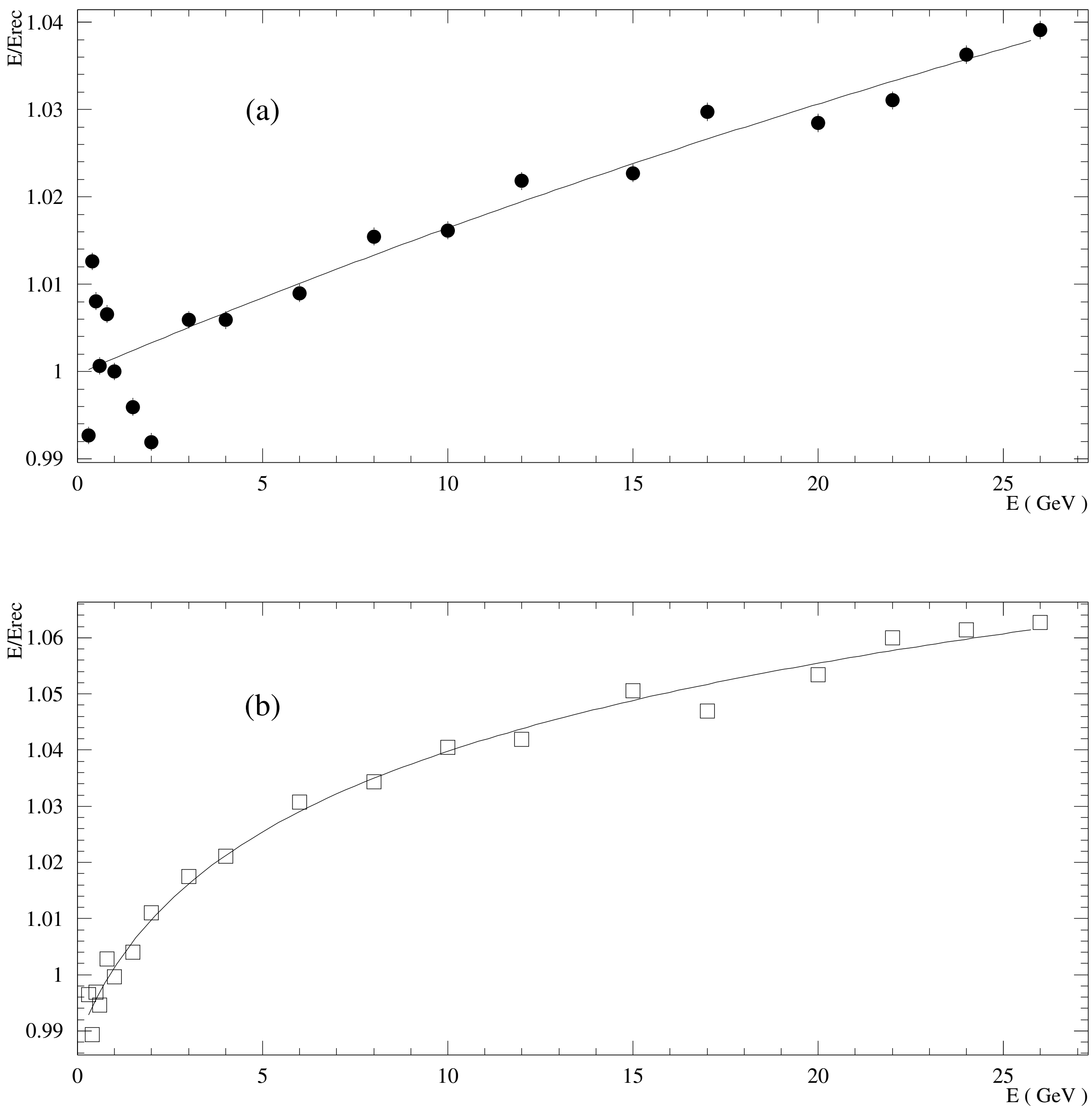

Figure 3: The mean longitudinal leakage from the EMC vs the energy of an incident electrons **(a)** and photons **(b)**.

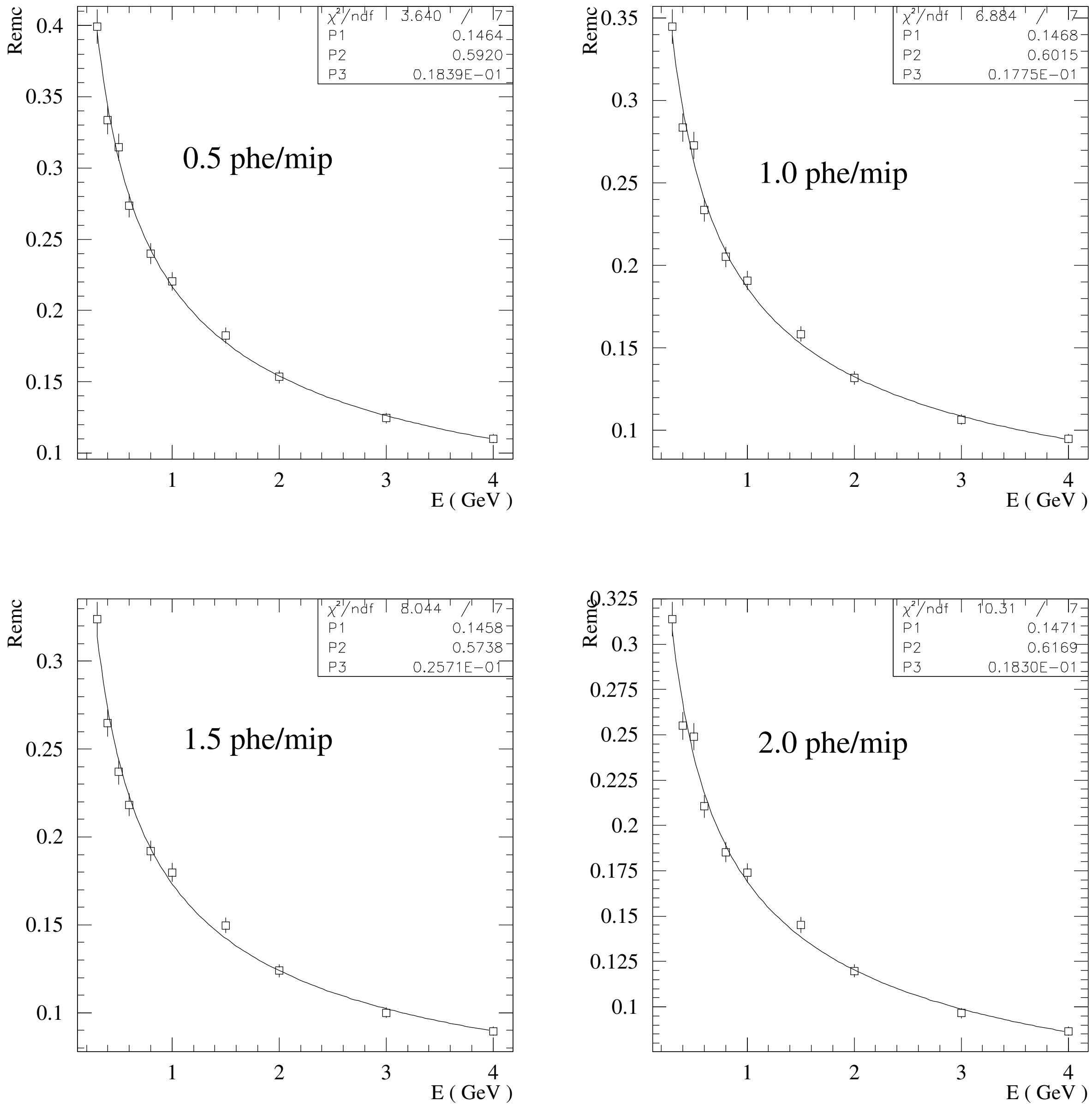

Figure 4: The mean EMC energy resolution for a different light yield from the tile/fiber assemblies. The $\boldsymbol{\sigma_{tot} = 0.1}$.

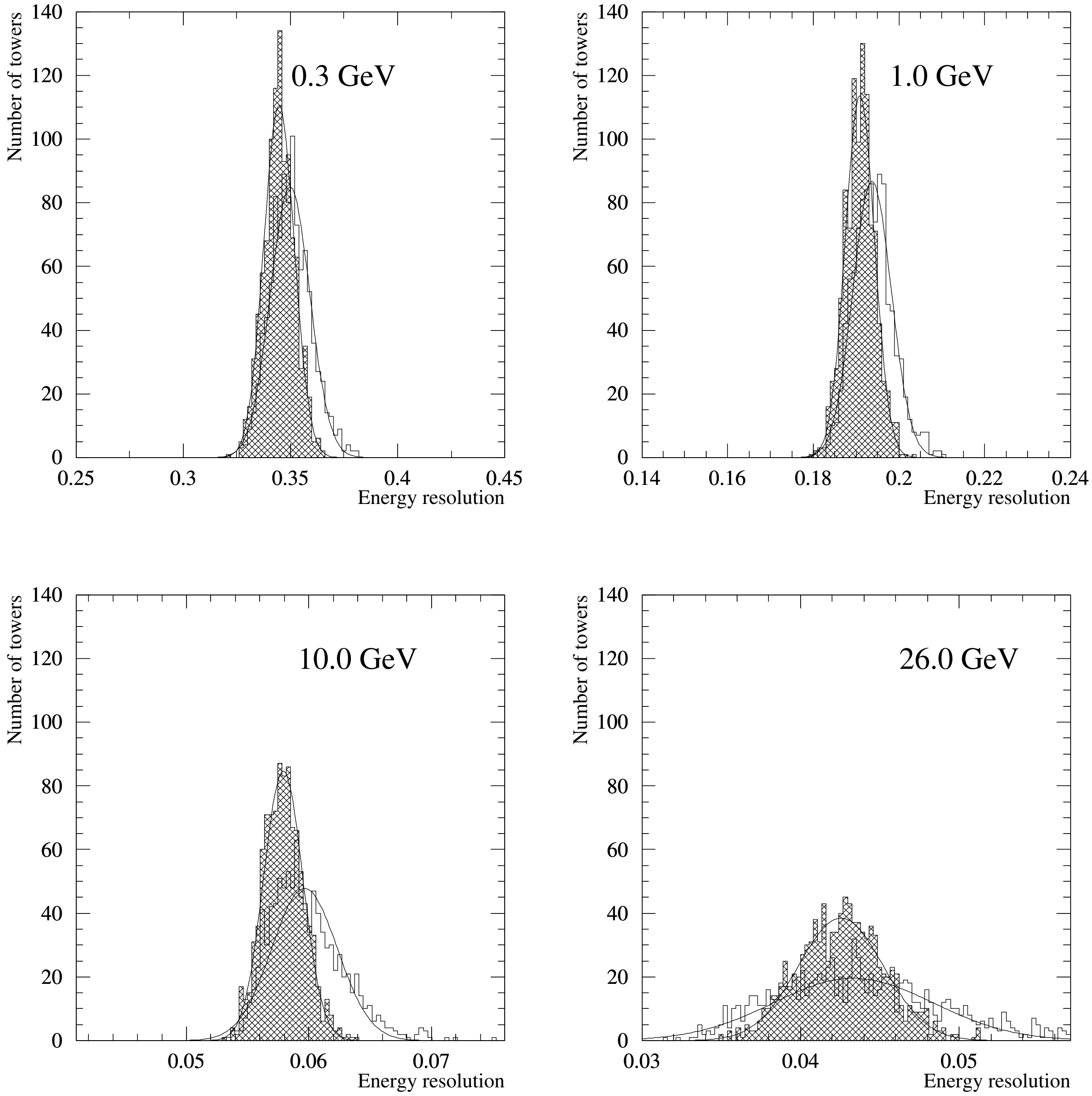

Figure 5: The distribution of the energy resolution for the whole EMC. The $\mathbf{N_{phe/mip} = 1.0}$, and the $\sigma_{\mathbf{tot}} = \mathbf{0.1}$ and $\mathbf{0.2}$ correspond to a hatched and unhatched histograms, respectively.

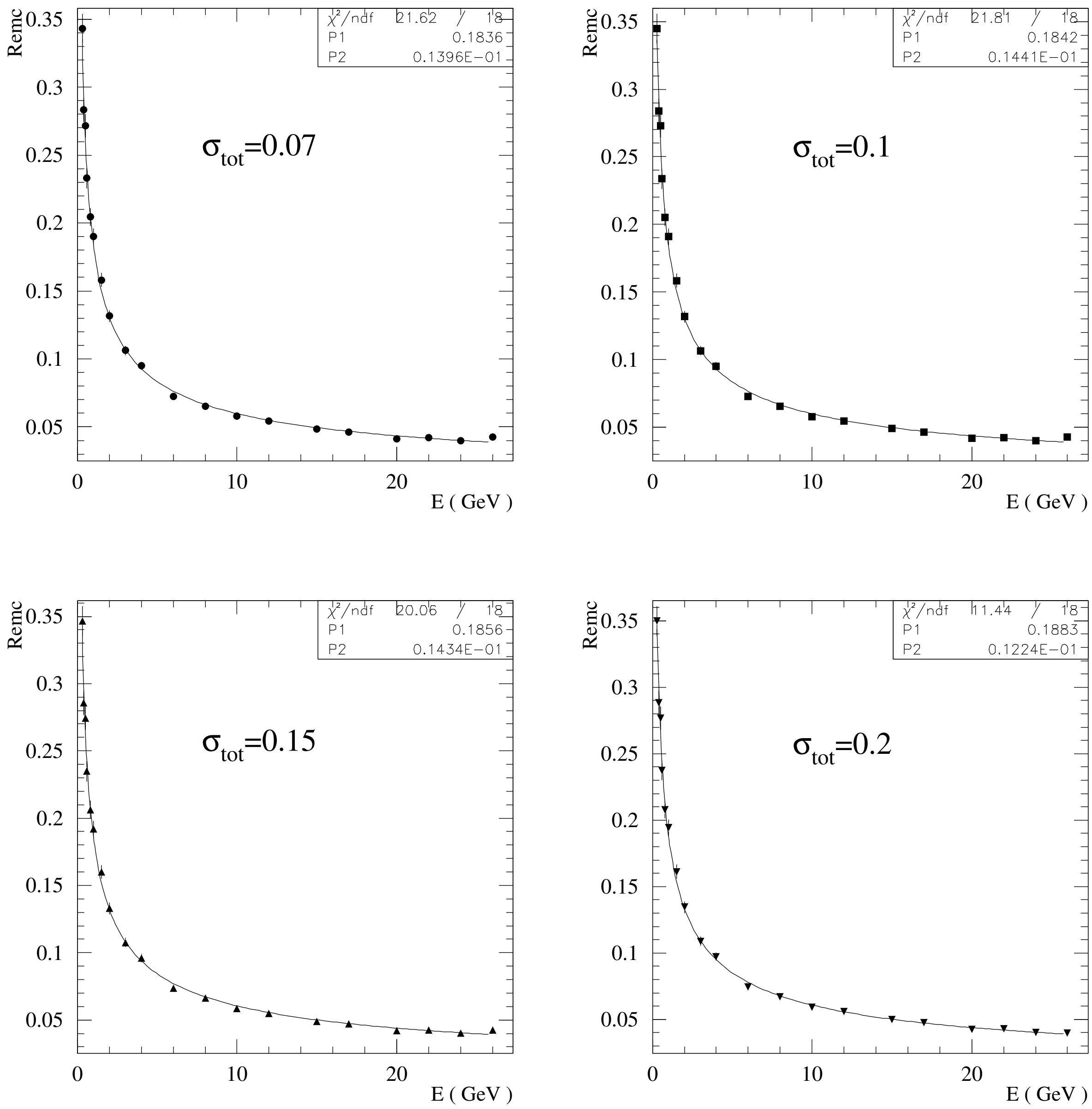

Figure 6: The mean EMC energy resolution for a different $\sigma_{\mathbf{tot}}$ and the $\mathbf{N_{phe/mip} = 1.0}$.

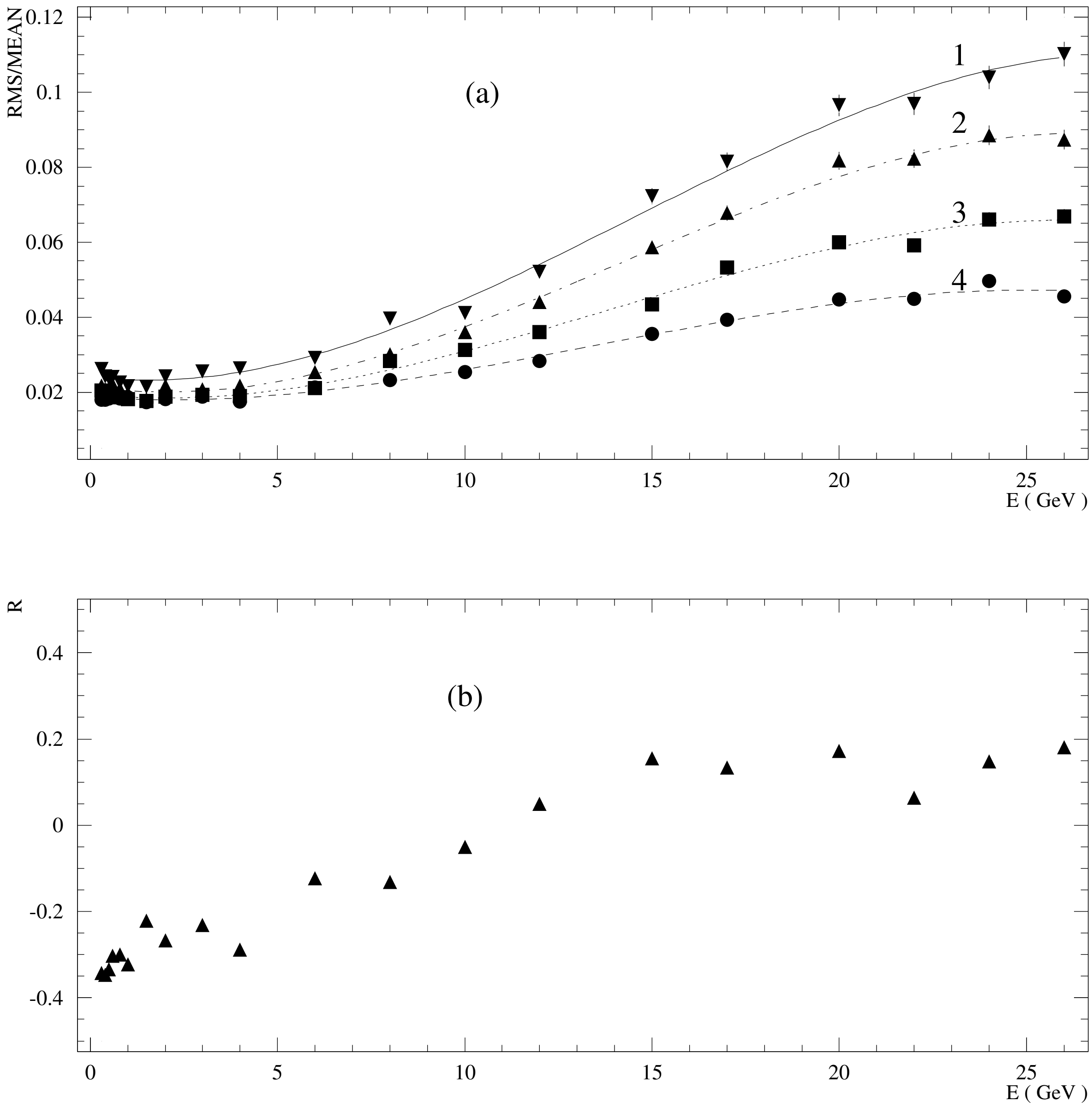

Figure 7: **(a).** The ratio of the sigma to the mean value of the distribution of a towers energy resolution. The $\mathbf{N_{phe/mip} = 1.0}$ and a **1, 2, 3, 4** correspond to $\sigma_{\mathbf{tot}}; \mathbf{0.2, 0.15, 0.1, 0.07}$, respectively. A curves are drawen for illustration, only. **(b).** The coefficient correlation **R** between the mean 'real signal' and the energy resolution of a EMC tower.

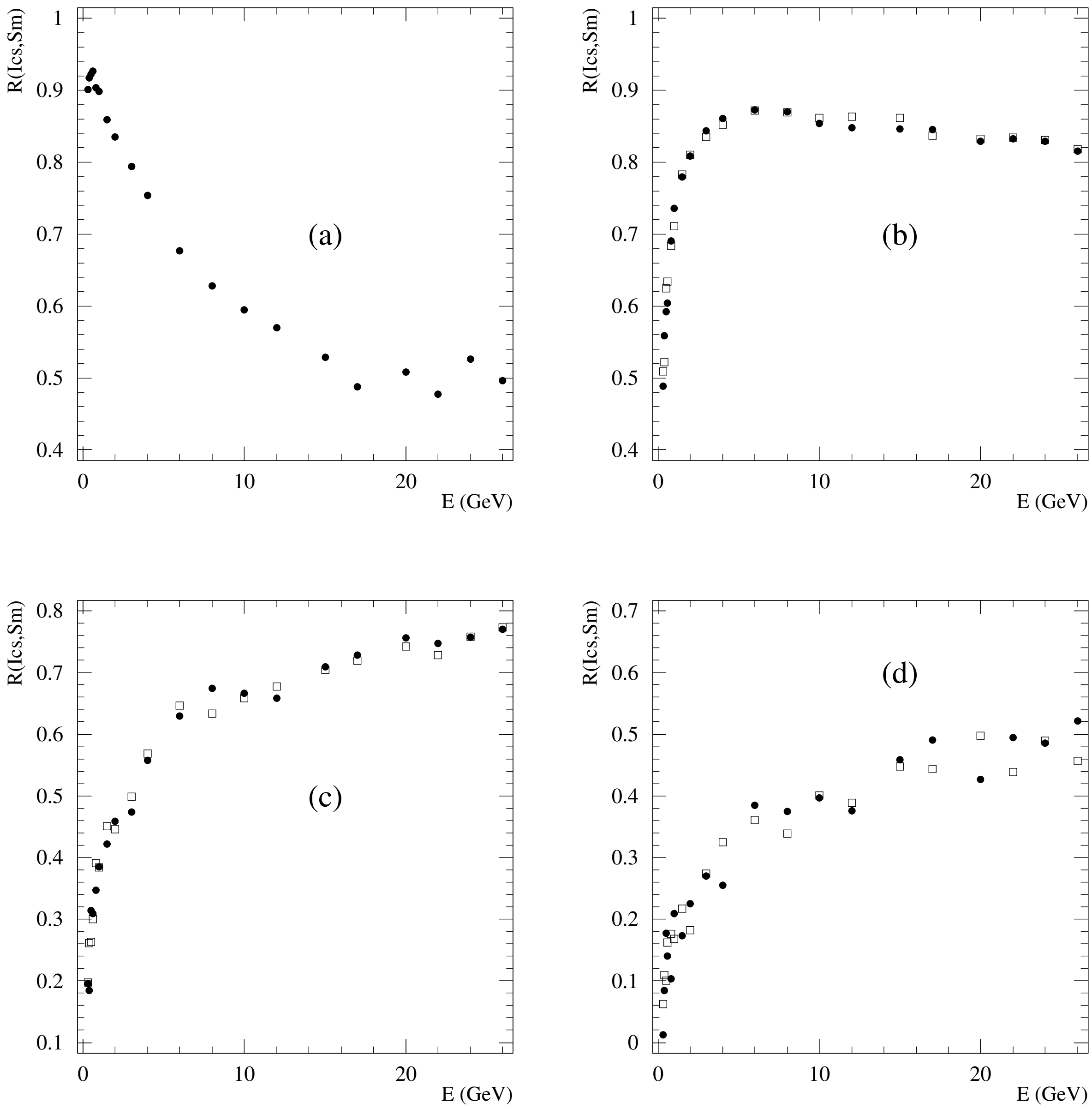

Figure 8: A dependence of the coefficient correlation **R(Ics,Sm)** between the mean 'real signal' from a tower **Sm** and the carrent indused by the ^{137}**Cs** source **Ics** vs. the energy of the incident electron, for a different location of the guide tube in the tower. The guide tube was incorporated into the lead plate number: **(a)** - 4, **(b)** - 7, **(c)** - 10, **(d)** - 13. A numeration of a plates was from the front surface of the tower. The $\sigma_{\mathbf{tot}} = \mathbf{0.07, 0.1}$ for a circles and squares, respectively.

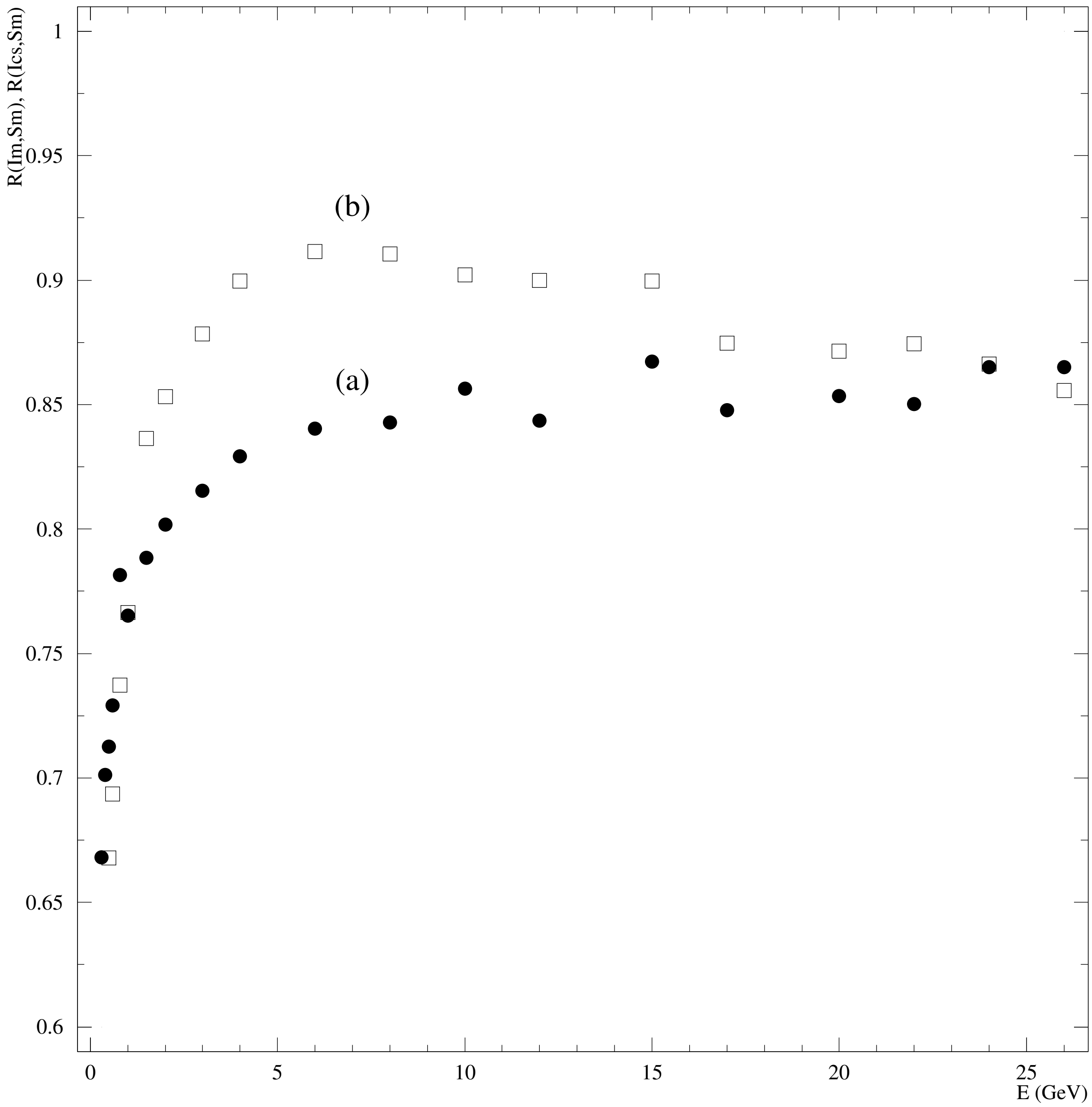

Figure 9: A dependence of the coefficient correlation **R(Im,Sm)** between the mean 'real signal' from a tower **Sm** and the signal from a muons **Im** vs. the energy of the incident electron - **(a)**, and the **(b)** - for the case of the ^{137}**Cs** calibration. A guide tubes were incorporated into the $\mathbf{6^{th}}$ and $\mathbf{7^{th}}$ lead plates of the EMC tower. The $\sigma_{\mathbf{tot}} = \mathbf{0.07}$.

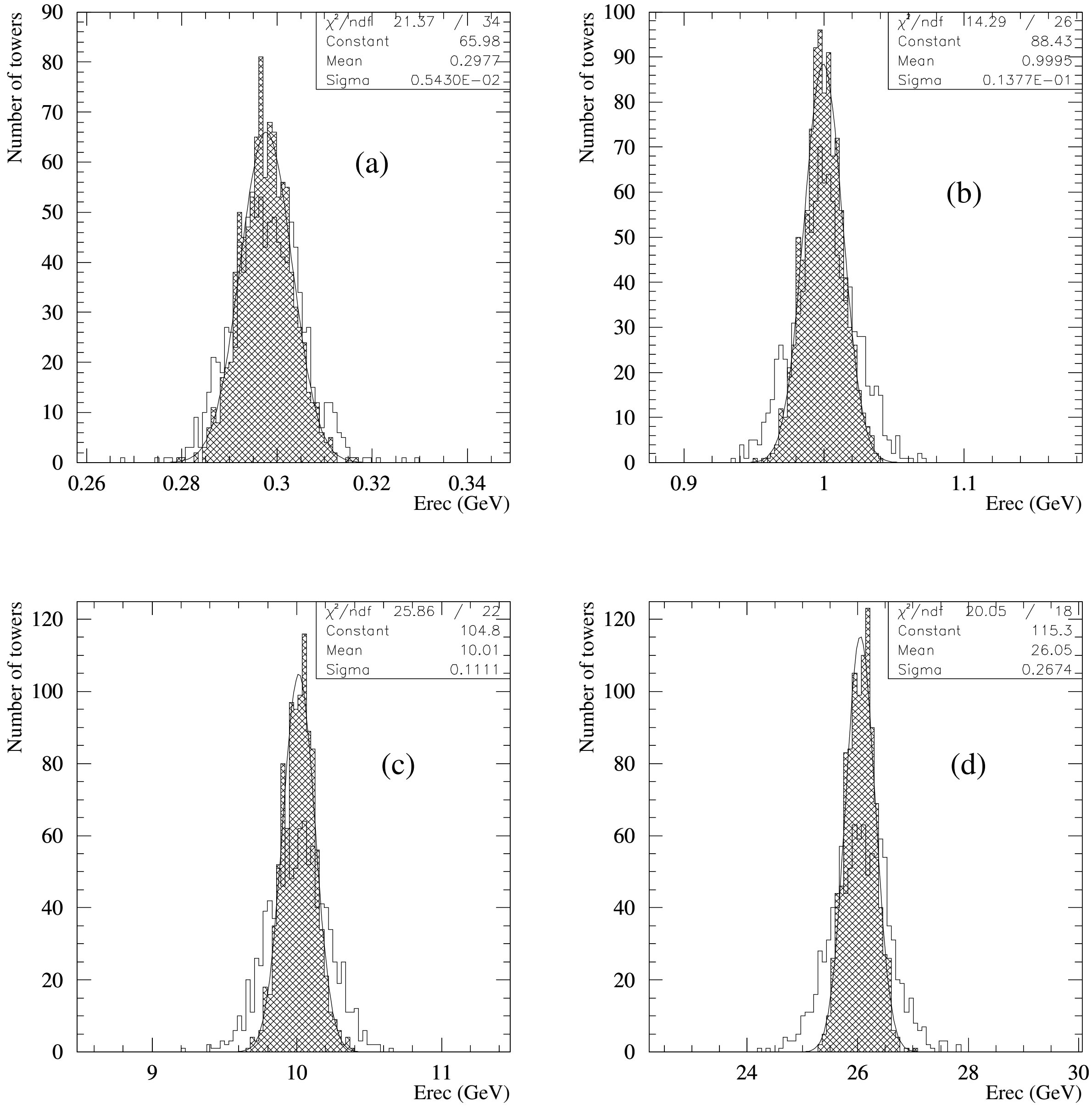

Figure 10: The distribution of the mean reconstructed energy **Erec** in the EMC towers with the correction by the cosmic ray muon calibration and withought this correction; a hatched and unhatched histograms, respectively. A **(a), (b), (c), (d)** correspond to the energy of the incident electron **0.3, 1.0, 10.0, 26.0 GeV**, respectively.

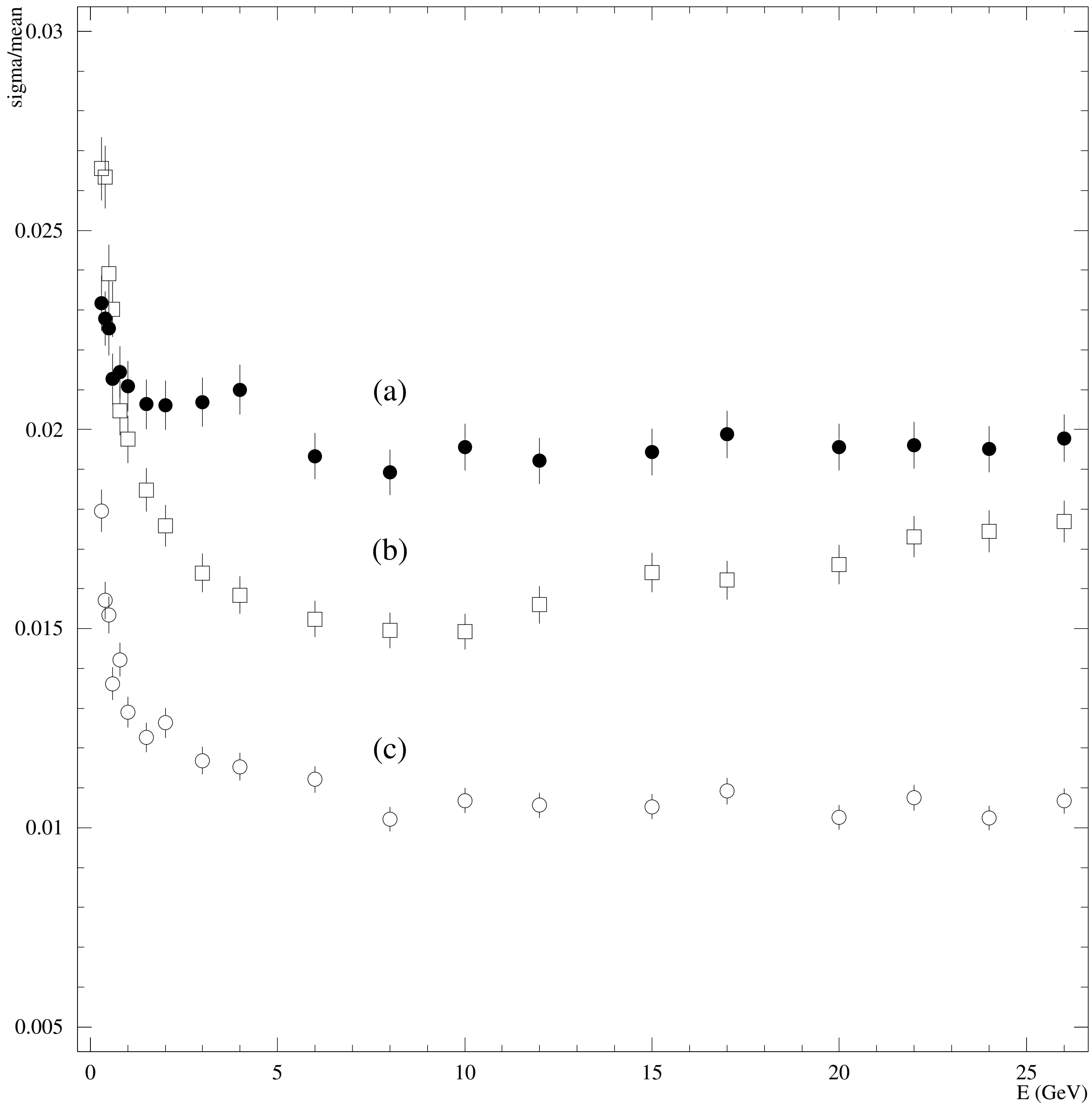

Figure 11: The dependence of the σ/μ of the distribution of the mean reconstructed energy in the EMC towers vs the energy of an incident electrons. A **(a)**, **(b)**, **(c)** correspond to the reconstruction procedure: withought any calibration, with the calibration from ^{137}**Cs** source, and with the calibration from a muons, respectively.

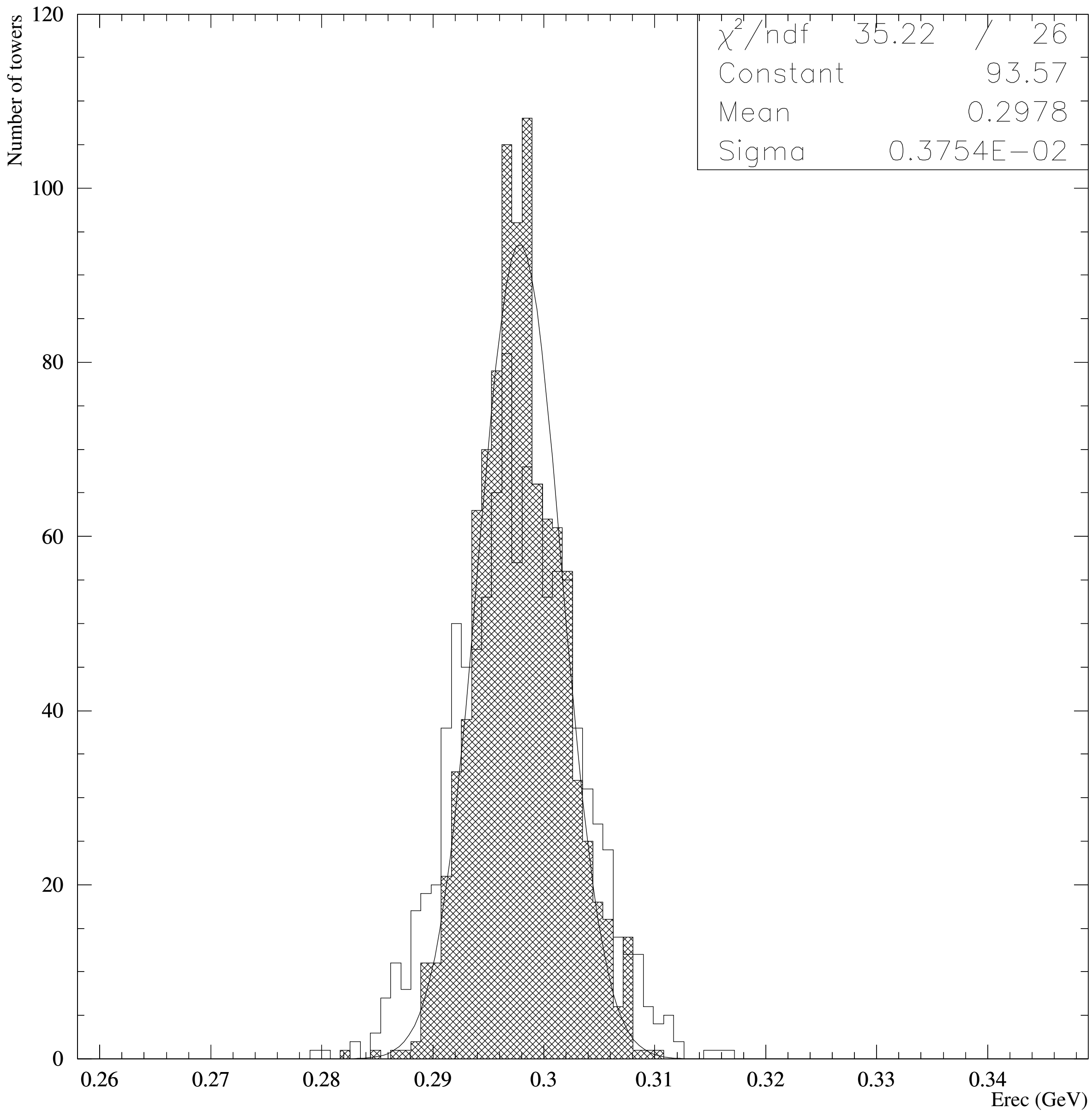

Figure 12: The distribution of the mean reconstructed energy **Erec** in the EMC towers with the correction by the ^{137}**Cs** source (the guide tube incorporated into the $\mathbf{4^{th}}$ lead plate) and with the correction by the muon calibration (unhatched). The energy of an incident electrons was 0.3 GeV.